Available online at www.sciencedirect.com
SCIENCE DIRECT®
Chemical Physics Letters 409 (2005) 129–133
CHEMICAL PHYSICS LETTERS
www.elsevier.com/locate/cplett

Faceting of Si nanocrystals embedded in SiO_2

Y.Q. Wang [a], R. Smirani [a], F. Schiettekatte [b], G.G. Ross [a,*]

[a] *INRS-EMT, 1650, Boulevard Lionel-Boulet, Varennes, Que., Canada J3X 1S2*
[b] *Université de Montréal, Lab. René J.A. Lévesque, Montréal, Que., Canada H3C 3J7*

Received 28 January 2005; in final form 25 April 2005
Available online 25 May 2005

Abstract

Faceting has been observed in some Si nanocrystals (Si nc) embedded in SiO_2 using high-resolution transmission electron microscopy (HRTEM). Statistical analyses of the interface-energy (Si nc/SiO_2) ratios for different facets of the single-crystalline Si nc have been carried out. For these single-crystalline Si nc, the interfacial energy ratios of {1 0 0} and {1 1 3} relative to {1 1 1} facets, are 1.1 and 0.89, respectively. The influences of planar defects such as twins and stacking faults on the faceting and interfacial energy of Si nc/SiO_2 are discussed in terms of their possible contribution to the interfacial energy.

Semiconductor surfaces are very interesting, not only because of their importance in the development of novel electronic devices, but also because of the wide variety of unexpected reconstructions that can occur during the growth process. Many researchers [1–3] are therefore motivated to investigate the surface energies of the bulk Si. As silicon becomes smaller and smaller, down to the nanoscale, the physical properties, especially the light-emitting property, change drastically. The optical properties of Si nanocrystals (Si nc) are affected by quantum confinement when their typical dimensions are similar to or smaller than the Bohr radius of the exciton, which in Si is of the order of 5 nm. This explains why most researchers focused their investigation on the Si nc smaller than 5 nm. However, the light-emitting property can be strongly influenced by the spatial confinement that promotes the electron hole recombination with radiative transition in the structures such as Si nanowires, whose dimensions (65 nm in width, 1 mm in length [4]) are much larger than the Bohr radius of excitons in Si (~4.5 nm). The spatial confinement is supposed to exist in the Si nc larger than 6 nm, and this stimulates us to carry out the microstructural characterization of the Si nc larger than 6 nm. Because of a well-defined wavelength luminescence, the well-controlled and large size Si nanostructures could be one of the most useful materials for light-emitting devices [4].

In this Letter, we report the observation of faceting in some Si nc (>6 nm) using high-resolution transmission electron microscopy (HRTEM). Statistical analyses of the interface-energy ratios for {1 0 0} and {3 1 1} facets, relative to {1 1 1} facets in the single-crystalline Si nc have been carried out. The influences of the planar defects such as twins and stacking faults on the faceting and interfacial energies are also discussed.

The Si nc were produced by a high-fluence (3×10^{17} cm^{-2}) implantation of 100-keV Si^+ into amorphous SiO_2 and annealing (1100 °C, 1 h). For a detailed experimental procedure, see [5]. The specimens for TEM examination were prepared in a cross-sectional orientation ([0 1 1] zone-axis for the Si substrate) using conventional techniques of mechanical polishing and ion-thinning. Dark-field imaging was carried out on a Philips CM30 microscope operating at 300 kV.

* Corresponding author. Fax: +1 450 929 8102.
E-mail address: ross@emt.inrs.ca (G.G. Ross).

0009-2614/$ - see front matter © 2005 Elsevier B.V. All rights reserved.
doi:10.1016/j.cplett.2005.04.108

HRTEM was performed using a JEOL JEM 2010 F scanning transmission electron microscope (STEM) operating at 200 kV and equipped with a Gatan imaging filter (GIF).

Fig. 1a shows a dark-field TEM image recorded using a (2 2 0) diffraction ring from the Si nc. From Fig. 1a, it can be clearly seen that a layer of Si nc is embedded in the SiO_2 film. The Si nc range from 2 to 22 nm in diameter, and there are three dominant groups (with average diameters of about 3, 6 and 12 nm, respectively) of nanocrystals in this specimen. To give reliable information on the general features of the faceting for the Si nc embedded in SiO_2, we recorded more than 200 nanocrystals and carried out a statistical analysis. For the Si nc smaller than 5 nm [5], most nanoparticles are spherical. For the Si nc larger than 6 nm, there are two dominant projected shapes along [0 1 1] direction: one being hexagonal; the other being elliptical or elongated. In the Si nc (~70%) ranging from 6 to 12 nm, faceting is dominant and many hexagonal-shape Si nc are observed; while in the Si nc with size larger than 10 nm [6], most are elliptical or elongated, although a few (1 0 0) facets are also observed. The size spectrum of the nanocrystals with the distribution of different shapes is summarized in Fig. 1b. In this Letter, we focus on the faceting investigation of the Si nc, and show some typical examples of faceting.

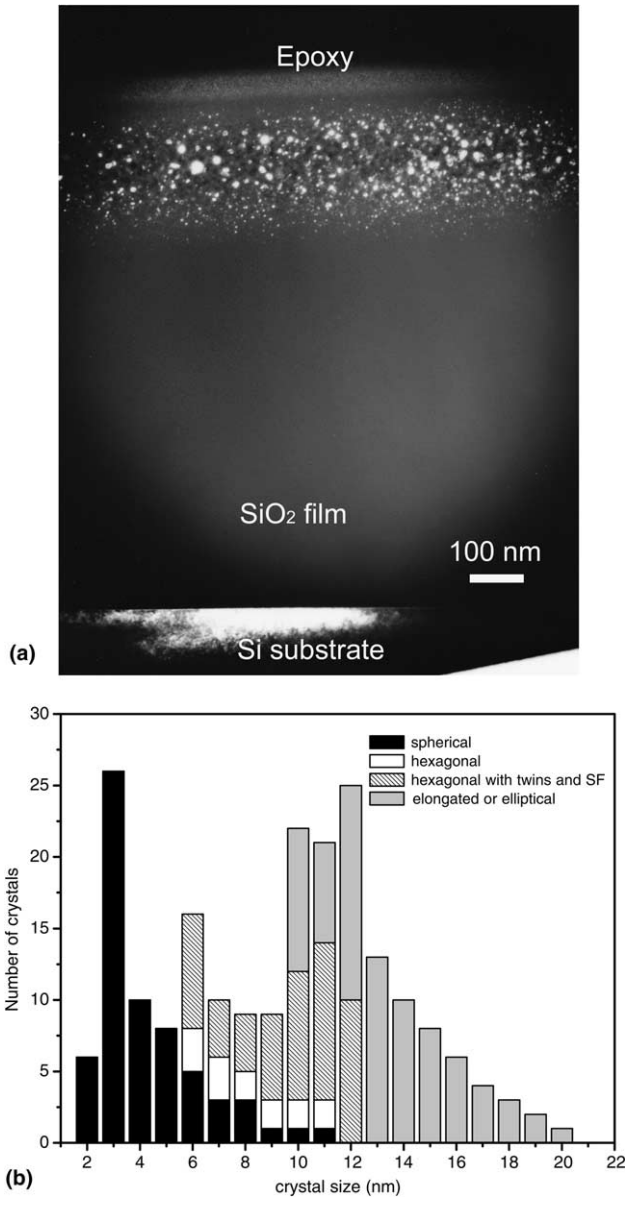

Fig. 1. (a) A typical dark-field image of the Si nc embedded in a 1-μm SiO_2 film; (b) the size spectrum of the Si nc with the distribution of different shapes.

Fig. 2 shows a [0 1 1] zone-axis HRTEM image of a single-crystalline Si nanoparticle with {1 1 1} and (1 0 0) facets. The projected shape of this nanoparticle is hexagonal (along the [0 1 1] direction), as indicated by the dashed lines in Fig. 2. Besides the {1 1 1} and (1 0 0) facets, {1 1 3} facets are also observed in some single-crystalline nanoparticles. Fig. 3a shows a [1 1 2] zone-axis HRTEM image of a single-crystalline Si nanoparticle with facets. The projected shape of this particle (along the [1 1 2] direction) is also more or less hexagonal (indicated by the dashed lines in Fig. 3a). This nanoparticle consists of $(11\bar{1})$ and {1 1 3} crystal facets. Therefore, a Wulff construction [7] can be reversed to estimate the ratios of the interfacial energies for the {1 1 1}, {1 0 0} and {1 1 3} facets of the single-crystalline Si nc. The schematic diagram of the Wulff construction is shown in Fig. 3b. Because the normal distance (r_i) from a common center to any given surface facet is

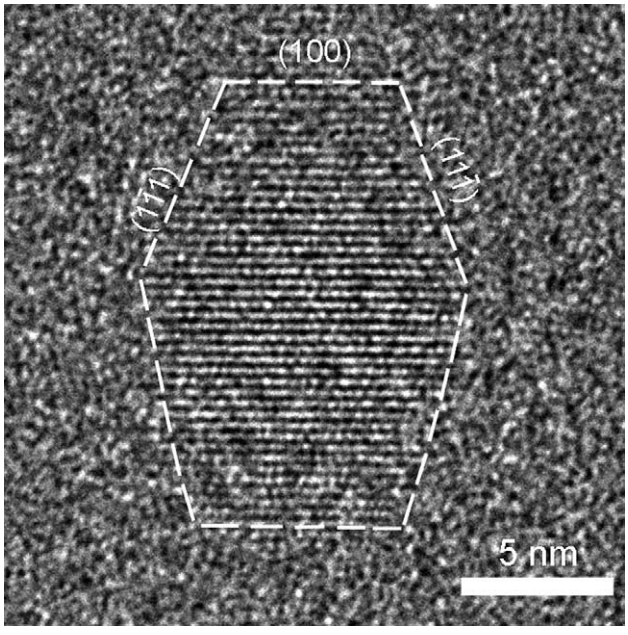

Fig. 2. [0 1 1] zone-axis HRTEM image of a typical single-crystalline Si nanocrystal, showing a hexagonal shape.

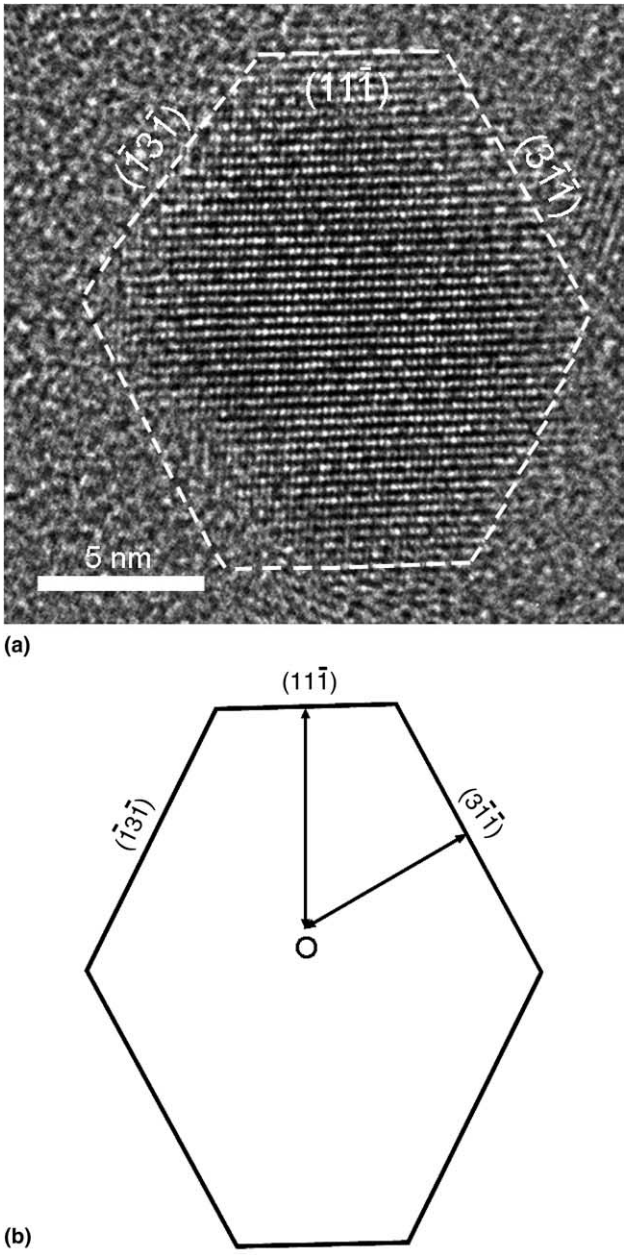

Fig. 3. (a) [112] zone-axis HRTEM image of a typical single-crystalline Si nanoparticle; (b) the schematic diagram of Wulff construction for the nanoparticle in (a).

proportional to the surface free energy (γ_i) of that facet [8], we can determine the relative ratio of interfacial energies by measuring the normal distance for the {111}, {100} and {113} facets of the single-crystalline Si nanoparticles, respectively.

The statistical results (obtained from 8 Si nc) of the relative ratios (±5%) of the normal distances [$r(i)$/$r(111)$] of the facets in the single-crystalline Si nc are summarized in Table 1. To estimate the surface energies for different facets, we need a known surface energy as a reference. Due to the great discrepancy of the surface

Table 1
The statistical results of the relative ratios (±5%) of the normal distances for the {111}, {100} and {113} facets in the single-crystalline Si nanoparticles

Facet	Relative ratio $r(i)/r(111)$
(111)	1
(100)	1.1
(311)	0.89

energy for {111} faces reported in the literature, and since there is no reliable value for the interfacial energy of Si nc/SiO_2, we report here the interface-energy ratios for different facets of Si nc and SiO_2, the same as those for the normal distance ratios for different facets in Table 1. From Table 1, we can deduce that the {113} facet has the lowest energy, which is in contradiction to the results obtained both from experiments and theoretical calculations. However, for the single-crystalline Si film, Gibson et al. [9] have shown that low-energy surfaces need not be confined to high-symmetry orientations and in particular that annealing of a Si(110) thin specimen causes extensive areas of Si(113) to be formed by faceting at the edges of the sample. Our observation proves that the {113} facets can have the lowest surface energy in the nanocrystalline Si.

Apart from the single-crystalline nanoparticles, the Si nc with twins and/or stacking faults are more frequently observed in this specimen. Fig. 4a shows the faceting in a typical Si nanoparticle with only a single-twin structure, and Fig. 5 shows an example of faceting in the Si nc with a twinning and stacking-fault structure. For the Si nc only with single-twin structures (Fig. 4a), the projected shape remains to be hexagonal, however, for those with twinning and stacking-fault structures (Fig. 5), the projected shape deviates slightly from a hexagon, being irregular in the lower-half particle. It can be seen from Fig. 4a that the top $(1\bar{1}1)$ plane, parallel to the twin plane, is significantly shorter than the $(11\bar{1})$ on the upper left side, or even than the (100) plane on the upper right side. Both nanoparticles have {111} and (100) facets, so the shape of the particles can be discussed in terms of the influences of the planar defects. The schematic diagram of the Wulff construction for a particle with a single twin is shown in Fig. 4b. The statistical results (obtained from 10 Si nc) of the relative ratios of the normal distances for different facets of the Si nc with defects are summarized in Table 2, which are equivalent to the interface-energy ratios for different facets.

Faceting is thermodynamically favorable to minimize the surface energy leading to an equilibrium shape. To determine whether these nanocrystals have reached the equilibrium shape, the effect of anneal time and temperature on the microstructure of the Si nc was also studied. For the Si nc annealed for more than 25 min, there is no

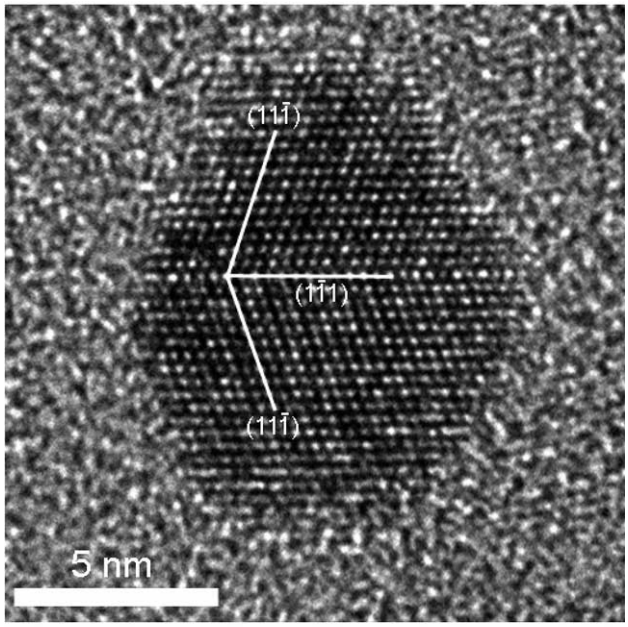

(a)

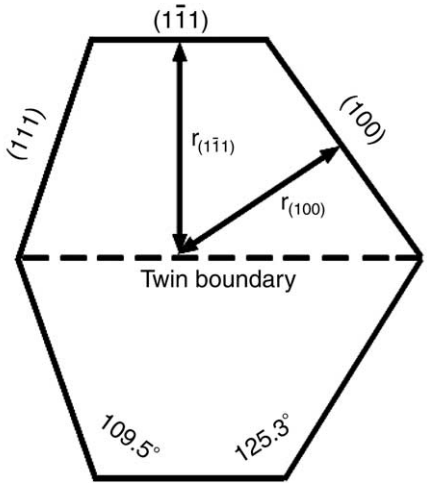

(b)

Fig. 4. (a) [0 1 1] zone-axis HRTEM image of a typical Si nanoparticle with a single-twin structure; (b) the schematic diagram of the Wulff construction for the nanoparticle in (a).

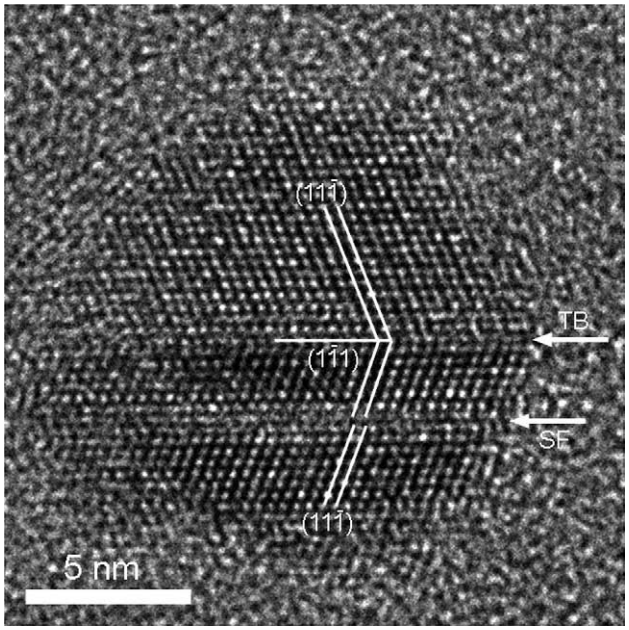

Fig. 5. An HRTEM image of a typical Si nanoparticle with nanotwin and stacking fault.

Table 2
The statistical results of the relative ratios (±5%) of the normal distances for {1 1 1} and {1 0 0} facets in the Si nanoparticles with planar defects

Facet	Relative ratio $r(i)/r(11\bar{1})$
(1$\bar{1}$1)	1
(11$\bar{1}$)	0.85
(1 0 0)	0.95

evident difference in the size and shape. Therefore, we conclude that the Si nc studied here have already reached the equilibrium shape.

For the Si nc smaller than 5 nm, most of the nanoparticles are spherical, and their projection shapes are circular. As the diameter of the Si nc increases, the differences in surface energy between the different crystallographic planes of Si nc become more significant. Thus, for the Si nc with size from 6 to 12 nm, (1 1 1), (1 0 0) and (1 1 3) facets become more stable, giving rise to the hexagonal shape. From our results, it can be seen that the order of the surface free-energy for the single-crystalline Si nc is: $\gamma_{(1\,1\,3)} < \gamma_{(1\,1\,1)} < \gamma_{(1\,0\,0)}$. Facets of {1 1 1} and (1 0 0) were also observed in the cross-section Si nanowires [10] with diameter of about 3.8 nm. For the Si nc with planar defects (as shown in Figs. 4a and 5), the surface energies of {1 1 1} planes are not equivalent any more. The plane parallel to the planar defects has a higher surface energy. One possible explanation is that the shape of the particle minimizes the interfacial energy including that of the twinning plane. Thus, even if {1 1 1} facets have a lower interfacial energy, as shown by single-crystalline particles, the parallel twinning plane comes with a higher cost, and the system adopts a shape that balances both contributions.

In conclusion, we have observed faceting in the Si nc (>6 nm) embedded in amorphous SiO_2 using HRTEM. Statistical analyses of the single-crystalline Si nc show the interface-energy (Si nc/SiO_2) ratios of {1 0 0} and {1 1 3} relative to {1 1 1} facets, are 1.1 and 0.89, respectively. The statistical analyses of the Si nc with defects indicate that the contribution of the interfacial energy associated with the planar defects inside the Si nc has to be considered, as they make the high-energy facets parallel to the twin plane shorter than those with lower interfacial energy.

Acknowledgments

This work has been supported by NanoQuébec and the Natural Science and Engineering Research Council of Canada (NSERC). HRTEM experiments were conducted using the TEM facility at Brockhouse Institute for Materials Research, McMaster University.

References

[1] J.H. Wilson, J.D. Todd, A.P. Sutton, J. Phys.: Condens. Matter 2 (1990) 10259.
[2] G.H. Gilmer, A.F. Bakker, Mater. Res. Soc. Symp. Proc. 209 (1991) 135.
[3] D.J. Eaglesham, A.E. White, L.C. Feldman, N. Moriya, D.C. Jacobson, Phys. Rev. Lett. 70 (1993) 1643.
[4] Y. Kanemitsu, H. Sato, S. Hihonyanagi, Y. Hirai, Phys. Stat. Sol. (a) 190 (2001) 755.
[5] Y.Q. Wang, R. Smirani, G.G. Ross, Nano Lett. 4 (2004) 2041.
[6] Y.Q. Wang, R. Smirani, G.G. Ross, F. Schiettekatte, Phys. Rev. B 71 (2005) 161310(R).
[7] C. Herring, in: C.R.G. Gommer, C.S. Smith (Eds.), Structure and Properties of Solid Surfaces, University of Chicago Press, Chicago, 1953.
[8] L.D. Marks, Rep. Prog. Phys. 57 (1994) 603.
[9] J.M. Gibson, M.L. McDonald, F.C. Unterwald, Phys. Rev. Lett. 55 (1985) 1765.
[10] Y. Wu, Y. Cui, L. Huynh, C.J. Barrelet, D.C. Bell, C.M. Lieber, Nano Lett. 4 (2004) 433.